Research Square

Preprints are preliminary reports that have not undergone peer review.
They should not be considered conclusive, used to inform clinical practice,
or referenced by the media as validated information.

Biocatalytic asymmetric radical alkene hydration

Thomas Ward

thomas.ward@unibas.ch

University of Basel https://orcid.org/0000-0001-8602-5468

Dongping Chen

university of basel https://orcid.org/0000-0002-1537-1539

Xiang Zhang

university of basel https://orcid.org/0009-0001-8977-6459

Article

Keywords:

Posted Date: January 28th, 2026

DOI: https://doi.org/10.21203/rs.3.rs-8642613/v1

License: This work is licensed under a Creative Commons Attribution 4.0 International License.
Read Full License

Additional Declarations: There is **NO** Competing Interest.

Biocatalytic asymmetric radical alkene hydration

Dongping Chen[1,2], Xiang Zhang*[1,2,3], and Thomas R. Ward*[1,2]

[1] Department of Chemistry, University of Basel, BPR 1096, Mattenstrasse 22, 4002 Basel, Switzerland.

[2] National Center of Competence in Research "Molecular Systems Engineering", 4058 Basel, Switzerland.

[3] Current address: Frontiers Science Center for Transformative Molecules, Shanghai Jiao Tong University, Shanghai, China.

Email: xiang.zhang@unibas.ch, thomas.ward@unibas.ch

Abstract

Asymmetric alkene hydration provides direct access to enantiopure alcohols and has been extensively developed through ionic mechanisms. Radical pathways remain largely unexplored, despite their potential for late-stage functionalization and functional-group tolerance. In this context, the Drago-Mukaiyama hydration—which proceeds via a metal–hydride hydrogen atom transfer (MHAT) mechanism—has found numerous applications in total synthesis, yet achieving high stereocontrol remains challenging. Here we show that cytochrome $P450_{BM3}$ can be repurposed as a radical hydratase that catalyzes the asymmetric radical hydration of both terminal and internal alkenes under aerobic conditions, affording a range of enantioenriched alcohols with up to 99% enantiomeric excess. Mechanistic investigations reveal a pathway initiated by metal–hydride hydrogen atom transfer (MHAT) and asymmetric intermolecular radical addition of dioxygen. A subsequent kinetic resolution of the hydroperoxide intermediate further upgrades the enantioselectivity of the alcohol product. This study highlights that radical alkene hydration can be catalyzed by haemoproteins, thus expanding the scope of challenging asymmetric reactions accessible to haemoproteins.

Introduction

Asymmetric alkene hydration offers a versatile means to synthesize value-added chiral alcohols from unfunctionalized alkenes[1,2]. In this context, several catalytic systems have been reported for the asymmetric hydration of alkenes. Achieving high stereocontrol relying on homogeneous catalysts remains challenging however[1]. Beyond small-molecule based catalysts, macromolecular systems have enabled asymmetric alkene hydration, including heterogeneous biopolymer-metal complexes[3-5], and DNA-based catalysts for activated alkenes[6]. By leveraging molecular recognition and stereocontrol, enzymes offer a promising route to asymmetric alkene hydration. Native hydratases, such as fatty acid hydratases, catalyze highly substrate-specific and stereoselective alkene hydration[7]. Enzyme-repurposing and decoy-molecule strategies have

been developed to extend biocatalytic asymmetric hydration to non-native alkene substrates[8-13]. Nonetheless, asymmetric alkene hydration remains dominated by ionic mechanisms, with radical pathways underexplored (Fig. 1a).

The Drago-Mukaiyama hydration is a versatile radical alkene hydration reaction[14-16], that has found broad applications in natural product synthesis (Fig. 1b)[17-19]. In 2014, Shenvi and coworkers were the first to explicitly connect the reaction mechanism to Halpern's metal–hydride hydrogen atom transfer (MHAT) hypothesis[20,21], a framework that has since been widely adopted to describe the Drago-Mukaiyama hydration process[18]. Here, an *in situ* generated metal–hydride moiety transfers an H-atom to the less-substituted carbon of the alkene, and the resulting carbon-centred radical then reacts with dioxygen to afford the Markovnikov hydration product. Stereocontrol in radical hydration remains elusive despite considerable effort, including chiral auxiliaries, leaving the asymmetric Drago-Mukaiyama hydration largely underdeveloped[22,23].

Enzymes, endowed with exquisitely well-structured secondary coordination spheres, catalyze challenging reactions with high stereocontrol[24-26]. Over the last two decades, the scope of enzymatic catalysis has expanded to include a range of new-to-nature transformations[27-34], enabled by strategies such as artificial metalloenzymes and enzyme repurposing[35-38]. In particular, metal–hydride chemistry, including MHAT reactions, has been smoothy integrated into biocatalysis to enable a variety of abiological asymmetric transformations[35,39-50]. For example, a non-haem iron/2-oxoglutarate-dependent enzyme was reported to catalyze the Drago-Mukaiyama hydration, although no stereoselectivity was achieved[39]. Incorporation of a biotinylated [Co(Schiff-base)] cofactor into an engineered chimeric streptavidin yielded an artificial radical cyclase for the synthesis of enantioenriched bicyclic terpenoid scaffolds via an MHAT mechanism[43]. Cobalt-protoporphyrin-derived artificial metalloenzymes have also been developed to catalyze non-natural MHAT reactions[48]. Native haemoproteins have been repurposed to catalyze asymmetric MHAT-based radical cyclizations and hydrogenations, respectively[46,47]. Building on these advances, we report the repurposing of cytochrome $P450_{BM3}$ as a hydratase that catalyzes asymmetric radical hydration of both terminal and internal alkenes. We surmise that an active-site Fe–H species reacts with an olefin via hydrogen-atom transfer, followed by intermolecular radical trapping with dioxygen to generate a peroxide intermediate, which subsequently undergoes an *in situ* reduction to afford enantioenriched alcohols (Fig. 1c). Taken together, these findings establish a biocatalytic platform for asymmetric radical alkene hydration and expand the scope of enzymatic metal–hydride chemistry.

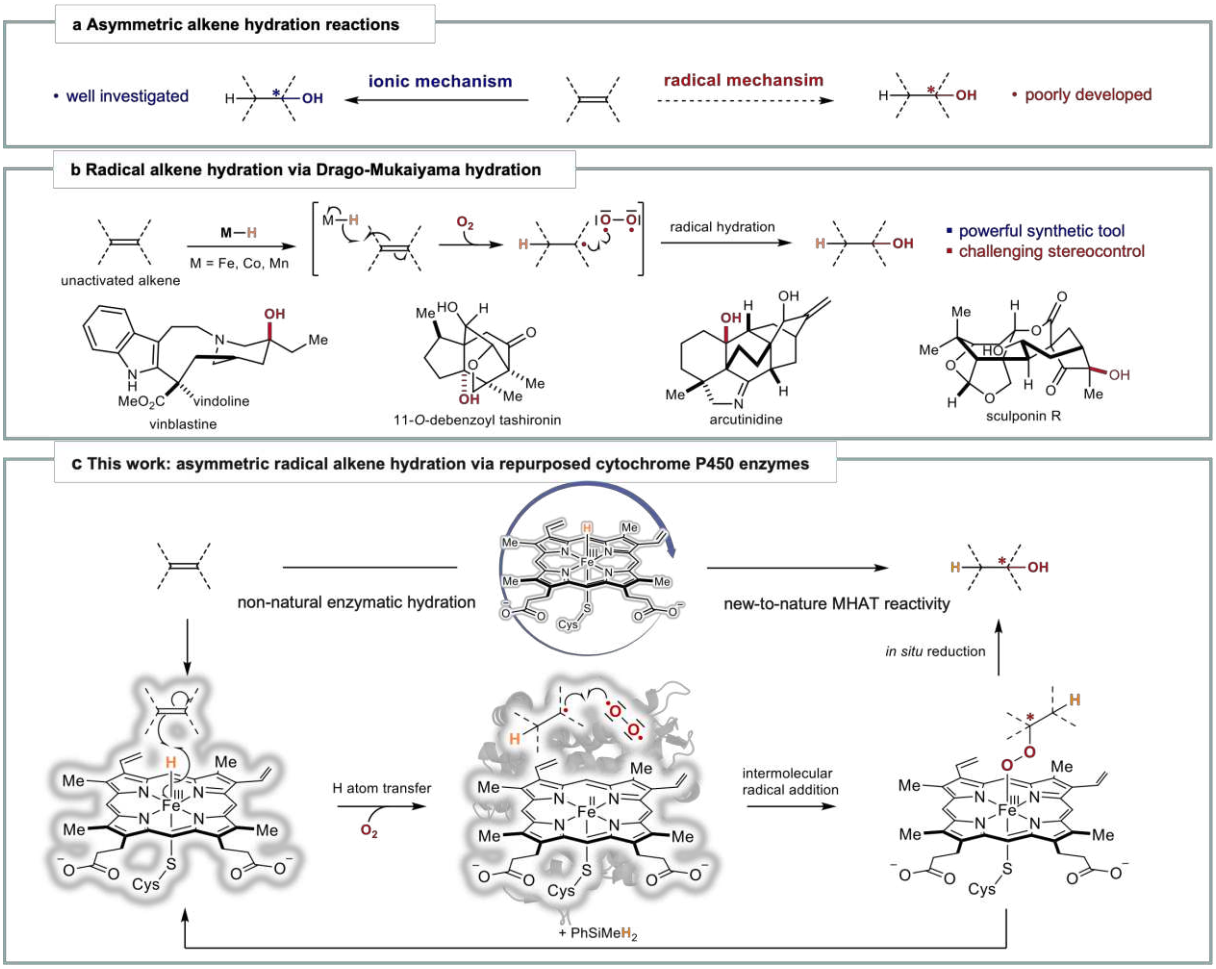


Fig. 1 | Asymmetric alkene hydration. a) Asymmetric alkene hydration proceeds predominantly through an ionic mechanism, while the alternative radical pathway remains largely underexplored. **b)** The Drago-Mukaiyama hydration—a radical alkene hydration reaction—has been applied in natural product synthesis. **c)** Our approach: repurposing cytochrome $P450_{BM3}$ as a radical hydratase for the asymmetric radical hydration of alkenes.

Results and discussion

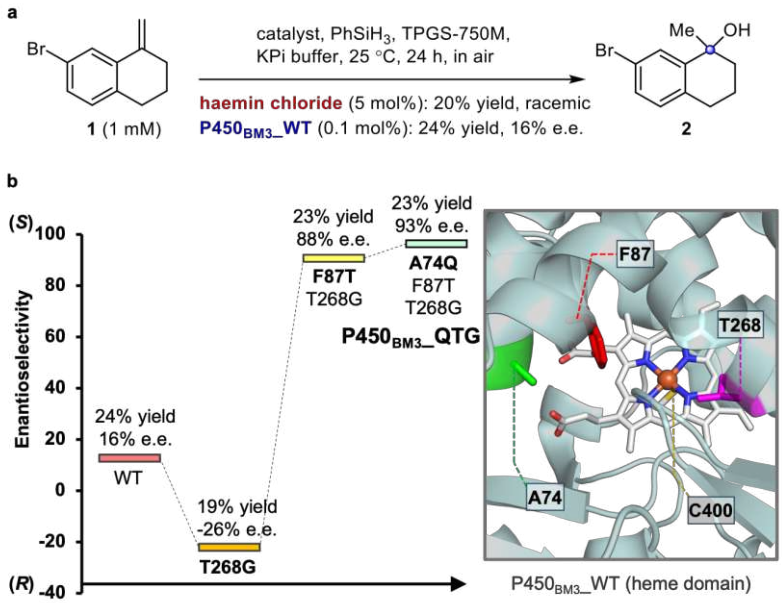
Development of a radical hydratase. Asymmetric alkene hydration reactions target primarily open-chain secondary alcohols, while cyclic tertiary alcohols such as tetralol **2** remain largely unexplored[3-6,8,10-13,22]. We therefore selected the alkene **1** for our preliminary studies, which features a bromide substituent for downstream synthetic manipulation. We envisioned that an H atom transfer (HAT) at the less-substituted olefinic carbon, followed by the radical addition of dioxygen within an enzyme's active site, should afford the enantioenriched tetralol **2** bearing a quaternary stereocenter. Inspired by our recent MHATase studies[43,46], we tested the reductase-deleted $P450_{BM3}$ for the radical hydration of alkene **1** in the presence of $PhSiH_3$ as hydride source and TPGS-750-M as surfactant. Sodium dithionite ($Na_2S_2O_4$) was included in the workup to reduce any unreacted peroxide intermediate to the corresponding alcohol **2** (Fig.

1c). The truncated P450$_{BM3}$_WT outperformed free haemin chloride for the radical hydration of alkene **1**, highlighting the beneficial effect of the hydrophobic environment provided by the metalloenzyme (Fig. 2a and Supplementary Table 1). Very modest enantioselectivity was observed for tetralol **2**, prompting us to apply directed evolution to optimize the performance of P450$_{BM3}$ as a radical hydratase.

Guided by the X-ray crystal structure of the P450$_{BM3}$ and the abundant evolutionary information reported for this enzyme[51], we applied iterative saturation mutagenesis, targeting amino acids lining the active site around the haem moiety (Fig. 2b). The mutant libraries were screened using *E. coli* whole cells, and the beneficial mutations were validated using purified P450$_{BM3}$ samples. A single mutation at position T268 (P450$_{BM3}$_T268G) led to the opposite enantiomer of tetralol **2**: the enantiomeric excess (e.e.) of tetralol **2** from 16% e.e. in favor of (*S*)-**2** using P450$_{BM3}$_WT, and 26% e.e. for (*R*)-**2** with P450$_{BM3}$_T268G. A second round of saturation mutagenesis at position F87 afforded a double mutant, P450$_{BM3}$_F87T-T268G, delivering (*S*)-**2** in 88% e.e. A third round of saturation mutagenesis yielded a triple mutant, P450$_{BM3}$_A74Q-F87T-T268G (P450$_{BM3}$_QTG hereafter), affording (*S*)-**2** in 93% e.e. and 23% yield (Supplementary Table 1). Mutations of the axial C400-residue led to poor catalytic performance, suggesting that the cysteine ligation is critical for the asymmetric radical alkene hydration (Supplementary Table 2).

Following whole-cell screening, we optimized key reaction parameters—using purified enzyme samples—to further improve the catalytic performance of the evolved radical hydratase, including the hydride source, enzyme loading, surfactant, and reaction time. A range of hydride sources were evaluated, including diverse silanes: $PhSiMeH_2$ performed best in terms of yield—particularly at lower loadings—while the e.e. remained unaffected (Supplementary Table 3). We surmise that this may be traced back to the improved water stability of $PhSiMeH_2$ compared to $PhSiH_3$[44,48,52]. Fine-tuning the $PhSiMeH_2$ concentration led to additional improvements in yield (Supplementary Table 4). Among various commercially-available non-ionic surfactants, TPGS-750-M afforded the best catalytic performance both in terms of activity and selectivity, and adjusting its concentration further improved the yield (Supplementary Tables 5-6). The biocatalyst loading of P450$_{BM3}$_QTG could be decreased to 0.2 mol% without compromising the yield and e.e. of tetralol **2** (Supplementary Tables 7-8). Based on these findings, the standard reaction was defined as follows: purified P450$_{BM3}$_QTG (0.2 mol %), $PhSiMeH_2$ (6 equiv. vs. alkene **1**) and TPGS-750-M (0.4 wt. %). Under these conditions, tetralol (*S*)-**2** was formed in 66% yield and 92% e.e., as quantified by SFC (Fig. 2c, entry 1). Both the absence of TPGS-750-M and the use of $PhSiH_3$ instead of $PhSiMeH_2$ negatively affected the

yield (Fig. 2c, entries 2-3). No tetralol **2** was detected in the absence of P450$_{BM3}$_QTG, supporting the hypothesis that the repurposed P450$_{BM3}$ indeed catalyzes the radical alkene hydration (entry 4). Moreover, no tetralol **2** was formed in the absence of $PhSiMeH_2$, consistent with the silane serving as the hydride source (entry 5). To unambiguously assign the absolute configuration of the tetralol **2**, we synthesized an enantiopure (*R*)-**2** sample via a reported sequence based on a Sharpless asymmetric dihydroxylation to access enantiopure (*R*)-**2** (Supplementary Figs. 1-2)[53,54].



c

Entry	Variations	Yield (%)	e.e. of (*S*)-2
1	Standard conditions	66	92%
2[a]	w/o TPGS-750M	33	88%
3[b]	w/ $PhSiH_3$ (6 eq.)	9	91%
4[c]	w/o P450$_{BM3}$_QTG	0	/
5[d]	w/o $PhSiMeH_2$	0	/

Fig. 2 | Directed evolution of a P450$_{BM3}$ radical hydratase for the asymmetric radical hydration of alkene 1 to enantioenriched tetralol 2. a) Initial investigation of free haemin chloride and P450$_{BM3}$_WT for the radical hydration of alkene **1**. **b)** Evolutionary trajectory of P450$_{BM3}$ radical hydratase for the asymmetric alkene hydration of alkene **1**, with beneficial amino acid positions highlighted in the crystal structure of P450$_{BM3}$_WT (haem domain, PDB: 2IJ2). Unless otherwise stated, the reaction conditions are: alkene **1** (1.0 mM), purified P450$_{BM3}$ variant (1 μM, 0.1 mol % catalyst loading), KPi buffer (50 mM, pH 7.0), $PhSiH_3$ (2 μL of 50 % v/v in DMSO, 20 equiv. compared with alkene **1**), TPGS-750-M (40 μL, from 2 wt. % in H_2O

stock solution), V_{tot} 400 µL, 25 °C in air for 24 h; workup by adding aq. $Na_2S_2O_4$ (10 µL, from 0.5 M in H_2O stock solution). Yield and e.e. were determined by SFC. Reactions were performed in duplicate. **c)** Reaction optimization with $P450_{BM3}$_A74Q-F87T-I268G ($P450_{BM3}$_QTG). The standard conditions are: alkene **1** (0.5 mM), purified $P450_{BM3}$_QTG (2 µM, 0.2 mol % catalytic loading), KPi buffer (50 mM, pH 7.0), $PhSiMeH_2$ (2 µL of 25 % v/v in DMSO, 6 equiv. compared with alkene **1**), TPGS-750-M (40 µL, from 4 wt. % in H_2O stock solution), V_{tot} 400 µL, 25 °C in air for 12 h; workup by adding aq. $Na_2S_2O_4$ (10 µL, from 0.5 M in H_2O stock solution). Yield and e.e. were determined by SFC. Reactions were performed in duplicates (for standard deviations, see Supplementary Table 9). [a] Milli-Q water (40 µL) was used instead of surfactant. [b]$PhSiH_3$ (2 µL of 15 % v/v in DMSO, 6 equiv. compared with alkene **1**) instead of $PhSiMeH_2$. [c]No $P450_{BM3}$_QTG added. [d]No $PhSiMeH_2$ added.

Substrate Scope. Next, we evaluated the substrate scope of the evolved $P450_{BM3}$_QTG variant under standard reaction conditions using 0.2 mol% biocatalyst loading (Fig. 3). Substrates bearing substituents at the C6, C7 or C8 positions were all well tolerated, affording a diverse array of functionalized tetralols **2**-**9** with a quaternary stereocenter in good to high e.e. Both electron-withdrawing and electron-donating substituents on the aromatic ring were compatible with the radical alkene hydration. The tetralols **10** and **11**, bearing two substituents on the phenyl ring, were obtained in good enantioselectivity. Beyond the tetralin motif, enantioenriched indanols **12** and **13** were also obtained: the bromoindanol **12** with a 99% e.e. Next, we evaluated structurally-diverse substrates to afford acyclic alcohol **14**, pyrrolidinol **15** and aliphatic secondary alcohols **16** and **17**. These products were formed with moderate to good enantioselectivity, although additional rounds of mutagenesis and reaction optimization were required to improve the catalytic performance to access alcohols **16** and **17**.

In addition to terminal alkenes, we tested internal alkenes for the asymmetric radical alkene hydration using $P450_{BM3}$_QTG as radical hydratase. A 1,2-disubstituted alkene was readily converted to tetralol **18** with good enantioselectivity. A range of trisubstituted alkenes were also smoothly converted, affording the tertiary alcohols **2**-**5**, **9**, **12** and **19**-**20** in good to high enantioselectivity. Importantly, the internal alkenes displayed the identical e.e. as the corresponding terminal alkenes (e.g. tetralols **2**-**5**, **9** and indanol **12**), consistent with a radical mechanism. In addition to endocyclic alkenes, trisubstituted exocyclic alkenes were converted to the corresponding tetralols **19** and **20** with good enantioselectivity. The more sterically-demanding tetrasubstituted alkene was also converted to tetralol **21** with excellent enantioselectivity, albeit with low diastereoselectivity. Finally, treatment of 1,4-

dihydronaphthalene **22** under standard catalytic conditions afforded two tetralols, **23** and **24**, with moderate to good enantioselectivity. The formation of tetralol **24** likely proceeds via a one-pot process in which hydrogen-atom transfer to the alkene generates a radical that subsequently migrates to a more stable benzylic position, followed by asymmetric radical addition of dioxygen.

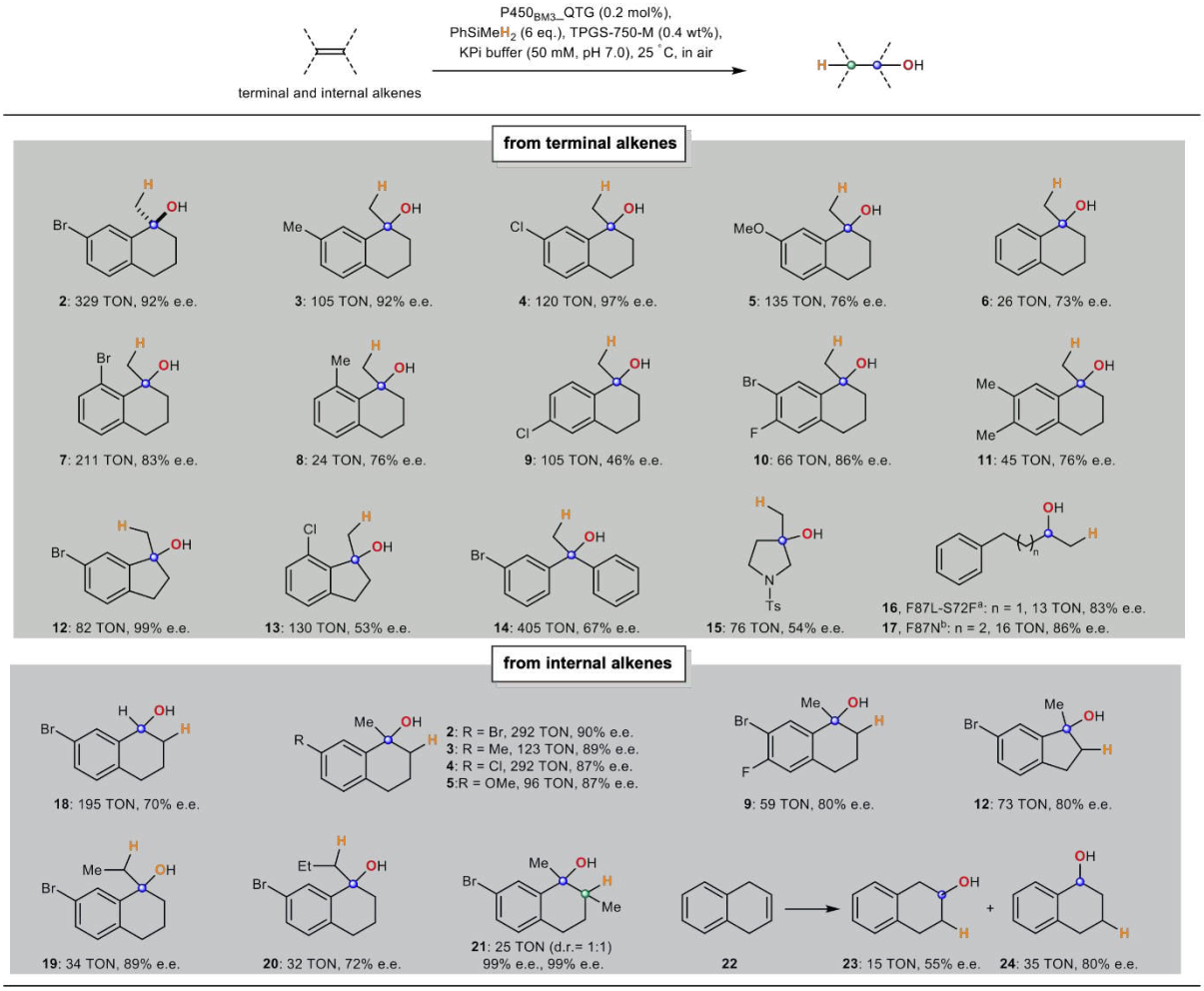


Fig. 3 | Substrate scope for the asymmetric radical alkene hydration catalyzed by the evolved P450$_{BM3}$. General procedure, unless otherwise stated: alkene substrate (1.0 mM), purified P450$_{BM3}$_QTG (2 μM, 0.2 mol % catalytic loading), KPi buffer (50 mM, pH 7.0), $PhSiMeH_2$ (2 μL of 25 % v/v in DMSO, 6 equiv. compared to the alkene substrate), TPGS-750-M (40 μL, from 4 wt. % in H_2O stock solution), V_{tot} 400 μL, 25 °C in air for 12 h; workup by adding aq. $Na_2S_2O_4$ (10 μL, from 0.5 M in H_2O stock solution). Yield and e.e. were determined by SFC, using 1,3,5-trimethoxylbenzene as internal standard (see the supplementary information for details). Reactions were performed in duplicate (for standard deviations, see Supplementary Fig. 3). [a]alkene substrate (1.25 mM), purified P450$_{BM3}$_QTG (12.5 μM, 1 mol % catalytic loading), $PhSiH_3$ (2 μL of 50 % v/v in DMSO, 16 equiv. compared with alkene

substrate), TPGS-1000-M (40 μL, from 2 wt. % in H_2O stock solution), 25 °C in air for 24 h. [b]alkene substrate (0.625 mM), purified $P450_{BM3}$_QTG (5 μM, 0.8 mol % catalytic loading), $PhSiH_3$ (2 μL of 50 % v/v in DMSO, 32 equiv. compared with alkene substrate), TPGS-1000-M (40 μL, from 2 wt. % in H_2O stock solution), 25 °C in air for 24 h. All alkenes used in the study are collected in Supplementary Fig. 36.

Mechanistic investigations. Motivated by the promising catalytic performance of the evolved radical hydratase, we set out to scrutinize the mechanism of the asymmetric radical hydration. We first carried out deuterium-labeling experiments to identify the source of the hydrogen atom added to the less-substituted alkene position in the hydration product (Fig. 4a). In the presence of $PhSiD_3$, the biocatalytic hydration of terminal alkene **1** and internal alkene **26** afforded tetralols **25** and **27**, respectively, with excellent enantioselectivity (Supplementary Figs. 4-8). In both cases, a single deuterium atom was incorporated exclusively at the less-substituted olefinic carbon, confirming that the silane serves as the hydrogen-atom source in the HAT pathway. This site-specific deuterium incorporation rules out an alkene isomerization prior to the radical hydration.

To further probe the mechanism of the biocatalytic alkene hydration, we carried out a radical-clock experiment using the cyclopropyl alkene substrate **28** and $PhSiMeH_2$ in the presence of $P450_{BM3}$_QTG (Fig. 4b). Under these conditions, the benzylic alcohol **29**, arising from cyclopropane ring opening of alkene **28**, was detected in 9% yield and 43% ee (Supplementary Figs. 9–10). This outcome is consistent with the reaction being initiated by hydrogen-atom transfer to the terminal alkene, generating the radical intermediate **Int-30**, which undergoes homolytic cyclopropane ring opening to form the benzylic radical **Int-31** prior to dioxygen addition. This proposed mechanism aligns with the radical MHAT pathway observed in our recent $P450_{BM3}$ MHATase study[46].

To determine the source of the oxygen atom in the hydration product, we performed ^{18}O-labeling experiments on alkene **1** using $^{18}OH_2$ (Fig. 4c, and Supplementary Figs. 11-17). Under aerobic conditions, tetralol **2** was obtained in 43% yield and 89% e.e. with no detectable ^{18}O-incorporation. Under anaerobic conditions, the combination of $PhSiMeH_2$ and $P450_{BM3}$_QTG did not afford any hydration product. These observations indicate that dioxygen serves as oxygen atom source in the biocatalytic asymmetric radical alkene hydration. Using $K_3[Fe(CN)_6]$ as an external oxidant under anaerobic conditions, tetralol **2** was obtained in 31% yield with incorporation of ^{18}O but with negligible enantioselectivity. We surmise that this outcome arises from oxidation of the carbon-centered radical intermediate to the corresponding cationic

intermediate by $K_3[Fe(CN)_6]$. This is consistent with the redox potentials of the benzylic radical and ferricyanide couples[55,56], followed by nucleophilic attack by $^{18}OH_2$ outside the enzyme's active site. Importantly, exposure of (*rac*)-epoxide **33** to the standard reaction condition with $PhSiMeH_2$ and $P450_{BM3}$_QTG afforded no alcohol **2**, thus ruling out a reductive epoxide opening as an alternative pathway to produce tetralol **2 (**Supplementary Figs. 18-19).

Next, we monitored the conversion of alkene **1** to tetralol **2** over time under our standard reaction conditions using $PhSiMeH_2$ and $P450_{BM3}$_QTG (Fig. 4d, and Supplementary Table 10). The yield of tetralol **2** increased steadily and reached a plateau after approximately 12 h, closely mirroring the consumption of alkene **1**. However, the overall mass balance, calculated as the sum of tetralol **2** and recovered alkene **1**, gradually eroded before stabilizing after ~24 h. Over the same period, the enantioselectivity of tetralol **2** increased from 68% to 92% e.e. Taken together, these observations suggest that the observed enantioselectivity does not arise solely from the initial C–O bond-forming step, and that the erosion in mass balance may reflect a concomitant kinetic resolution that preferentially consumes the minor enantiomer of tetralol **2**[34].

The observed decrease in mass balance prompted us to examine the presence of byproducts formed during the biocatalytic radical hydration of alkene **1** (Fig. 4e, and Supplementary Figs. 20-26). Gas chromatography-mass spectrometry (GC-MS) analysis revealed the formation of a bis-hydroxylated product derived from alkene **1**. A preparative-scale reaction with alkene **1** afforded diol **34** in 28% yield with a diastereomeric ratio of 1.5:1 (58% e.e. for the major diastereomer and 81% e.e. for the minor diastereomer); its retention time matched that of the previously detected species in the GC-MS analysis. NMR characterization of diol **34** revealed the presence of an additional hydroxy-group at the benzylic C4-position relative to tetralol **2**. The identity of diol **34** was further confirmed by comparison with an independently-synthesized authentic sample. Accounting for the amount of diol **34** formed over the course of the reaction resulted in an excellent mass balance, confirming that diol **34** is the major byproduct formed under the reaction conditions.

Next, we set out to investigate the pathway leading to formation of diol **34** during the biotransformation (Fig. 4e). When (*rac*)-tetralol **2** was subjected to standard reaction conditions, no diol **34** was observed: only tetralol **2** was recovered. This suggests that diol **34** is not formed directly from the hydration product **2** (Supplementary Fig. 27). Importantly, when a lower $P450_{BM3}$_QTG-enzyme loading was used, and without addition of $Na_2S_2O_4$ prior to workup, the hydroperoxide intermediate **35** was detected by high-performance liquid chromatography

(HPLC) in high e.e. but low yield (Fig. 4f, and Supplementary Figs. 28-30). The retention time and corresponding UV-Vis trace of the hydroperoxide **35** matched that of an independently-synthesized hydroperoxide sample[57]. The high e.e. of the hydroperoxide **35** prompted us to examine whether it participates in the kinetic resolution to afford the diol **34** side-product (Supplementary Figs. 31-35). Independent experiment using (*rac*)-hydroperoxide **35** as substrate in the presence of $PhSiMeH_2$ and $P450_{BM3}$_QTG revealed the formation of diol **34** in 34% yield. In this reaction, the hydroperoxide **35** was recovered in 37% yield with 88% e.e., confirming a kinetic resolution process leading to the enrichment of the major enantiomer of (*S*)-**2**. Notably, in the absence of $PhSiMeH_2$, conversion of hydroperoxide **35** to diol **34** still proceeded, suggesting that the Fe–H species is not involved in this process. Cytochrome P450 enzymes have been reported to react with hydroperoxides in the absence of reductant, catalyzing intramolecular oxygen-transfer reaction via a ferryl moiety[58-60]. Accordingly, we hypothesize that $P450_{BM3}$_QTG functions as an intramolecular peroxygenase with hydroperoxide **35** functioning both as hydroperoxide source and substrate, catalyzing intramolecular hydroxylation at the benzylic C4 position to generate diol **34**. The selectivity factor for this kinetic resolution with $P450_{BM3}$_QTG alone was determined as $s = 45$, favoring the reaction of (*R*)-**35** and thus affording the enantioenriched (*S*)-**35** (Supplementary Table 11). Taken together, these results reveal a kinetic resolution of the hydroperoxide intermediate formed in the radical hydration process, thus contributing to upgrade the e.e. of tetralol **2**. The evolved $P450_{BM3}$_QTG thus functions as a bifunctional enzyme in the asymmetric radical hydration, acting both as a radical hydratase featuring an Fe–H species and as a peroxygenase involving an Fe=O ferryl species (Supplementary Fig. 35)

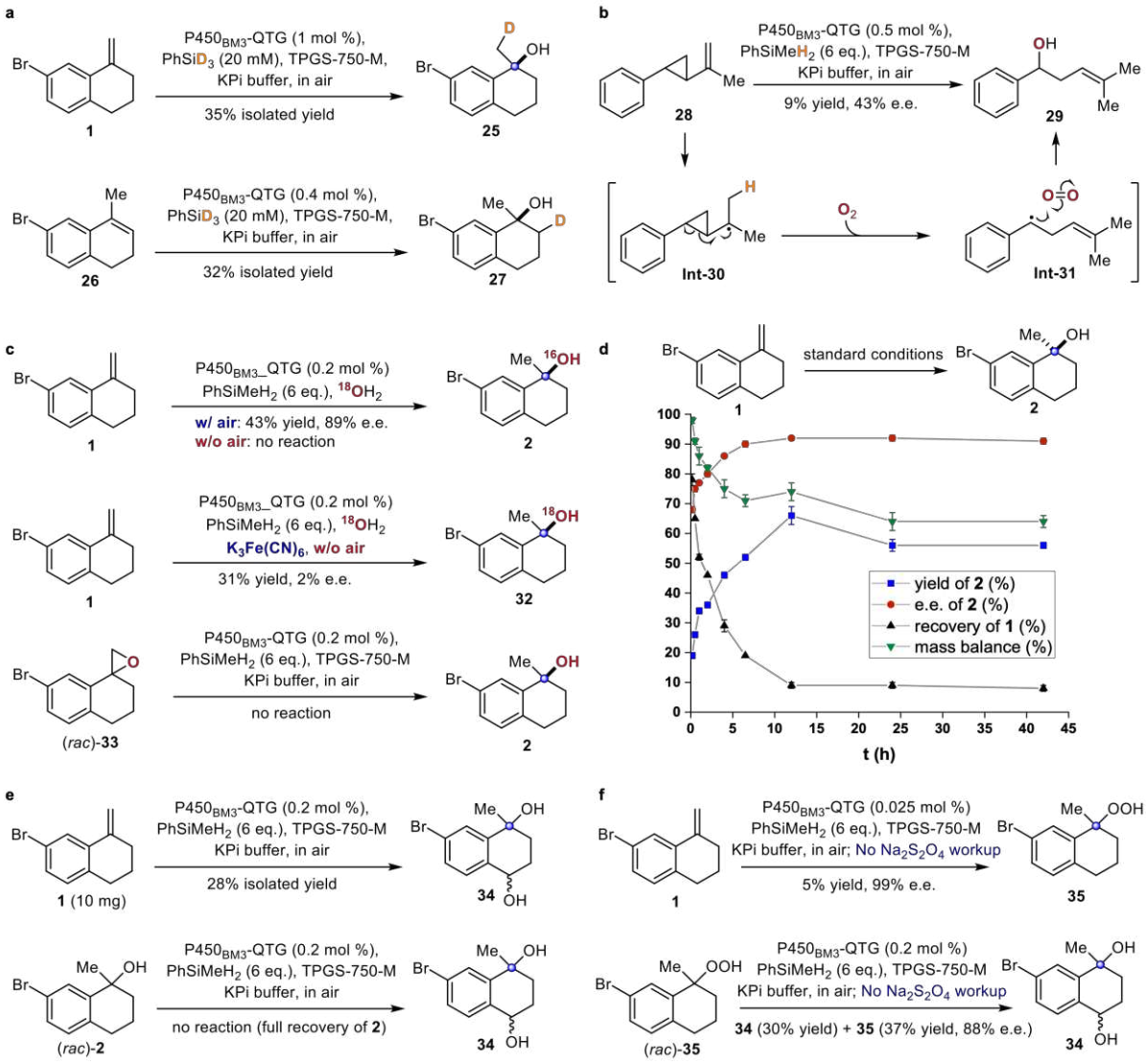


Fig. 4 | Mechanistic studies of the P450$_{BM3}$_QTG-catalyzed radical alkene hydration. **a)** Deuterium-labeling studies of terminal alkene **1** and internal alkene **26** using $PhSiD_3$. **b)** Radical-clock experiment with cyclopropyl alkene **28** in the presence of P450$_{BM3}$_QTG and $PhSiMeH_2$, supporting a radical pathway. **c)** Origin of the incorporated oxygen atom probed by ^{18}O-labeling and epoxide-opening experiments. **d)** Time-course analysis of the conversion of alkene **1** to tetralol **2**, highlighting the yield of **2** (blue), e.e. of **2** (red), recovery of **1** (black), and mass balance (green). **e)** Analysis of the reaction mixture revealing formation of diol **34** as the major byproduct. **f)** Detection of hydroperoxide **35** as substrate for the formation of diol **34** (see the proposed mechanism in Supplementary Fig. 35).

Conclusion

Radical alkene hydration, epitomized by the Drago-Mukaiyama hydration, remains underexplored in asymmetric catalysis. Haemoproteins have emerged as a versatile catalytic platform for various new-to-nature transformations, including radical MHAT catalysis, offering excellent stereocontrol in challenging bond-forming process[27,28,34,36,44,46,47]. Herein, we

repurposed cytochrome $P450_{BM3}$ as a radical hydratase that catalyzes asymmetric alkene hydration via an MHAT-initiated radical pathway. Through three rounds of directed evolution, we identified an optimal variant, $P450_{BM3}$_QTG, which catalyzes the asymmetric radical hydration of a range of terminal and internal alkenes under aerobic conditions in the presence of $PhSiMeH_2$. This biotransformation provides access to diverse enantioenriched cyclic tertiary alcohols bearing a quaternary stereocenter, a class of products that is less-developed in current asymmetric alkene hydration. Mechanistic studies support an MHAT radical mechanism in which the silane serves as the hydrogen atom donor and dioxygen as the oxygen atom source. We further uncovered a kinetic resolution pathway of the hydroperoxide intermediate formed during the hydration process—in which the minor enantiomer is preferably converted into a diol byproduct through biocatalytic intramolecular hydroxylation—thereby upgrading the enantioselectivity of the final alcohol. These findings expand the landscape of asymmetric alkene hydration and abiological radical biocatalysis, opening fascinating perspectives for the biocatalytic production of diverse enantioenriched fine chemicals.

ACKNOWLEDGEMENTS

T. R. W. thanks the National Centre of Competence in Research (NCCR) Catalysis (grant no. 180544) and Molecular Systems Engineering (grant no. 200021_178760) for funding. We acknowledge Dr. Tsvetan Kardashliev for biological support.

AUTHOR CONTRIBUTIONS

T. R. W., D. C. and X. Z. conceived and designed the study. D. C. contributed to the directed evolution of $P450_{BM3}$ radical hydratase and the development of substrate scope. X. Z. performed the optimization of reaction conditions and improved the performance of substrate scope. D. C. and X. Z. contributed equally to the mechanistic studies. D. C. and X. Z. performed the catalytic experiment and recorded the data. T. R. W., D. C. and X. Z. analyzed the data. T. R. W., D. C. and X. Z. wrote the manuscript. All authors have given approval to the final version of the manuscript.

References

1 Kennemur, J. L., Maji, R., Scharf, M. J. & List, B. Catalytic asymmetric hydroalkoxylation of C–C multiple bonds. *Chem. Rev.* **121**, 14649–14681 (2021).

2 Demming, R. M., Fischer, M.-P., Schmid, J. & Hauer, B. (De)hydratases—recent developments and future perspectives. *Curr. Opin. Chem. Biol.* **43**, 43–50 (2018).

3 Zhang, X., Li, Y.-J., Huang, M.-Y. & Jiang, Y.-Y. Asymmetric hydration of allyl alcohol catalyzed by polysulfostyrene–gelatin–Co complex. *Polym. Adv. Technol.* **13**, 305–309 (2002).

4 Xue, L. *et al.* The asymmetric hydration of 1-octene to (S)-(+)-2-octanol with a biopolymer–metal complex, silica-supported chitosan–cobalt complex. *React. Funct. Polym.* **58**, 117–121 (2004).

5 Wang, S.-Q. *et al.* A novel efficient route for preparation of chiral β-hydroxycarboxylic acid: Asymmetric hydration of unsaturated carboxylic acids catalyzed by heterobimetallic complex wool–palladium–cobalt. *J. Mol. Catal. A Chem.* **264**, 60–65 (2007).

6 Boersma, A. J. *et al.* Catalytic enantioselective syn hydration of enones in water using a DNA-based catalyst. *Nat. Chem.* **2**, 991–995 (2010).

7 Engleder, M. & Pichler, H. On the current role of hydratases in biocatalysis. *Appl. Microbiol. Biotechnol.* **102**, 5841–5858 (2018).

8 Wuensch, C. *et al.* Asymmetric enzymatic hydration of hydroxystyrene derivatives. *Angew. Chem. Int. Ed.* **52**, 2293–2297 (2013).

9 Payer, S. E., Pollak, H., Glueck, S. M. & Faber, K. A rational active-site redesign converts a decarboxylase into a C═C hydratase: "Tethered acetate" supports enantioselective hydration of 4-hydroxystyrenes. *ACS Catal.* **8**, 2438–2442 (2018).

10 Demming, R. M. *et al.* Asymmetric enzymatic hydration of unactivated, aliphatic alkenes. *Angew. Chem. Int. Ed.* **58**, 173–177 (2019).

11 Engleder, M. *et al.* Evolving the promiscuity of elizabethkingia meningoseptica oleate hydratase for the regio- and stereoselective hydration of oleic acid derivatives. *Angew. Chem. Int. Ed.* **58**, 7480–7484 (2019).

12 Gajdoš, M. *et al.* Chiral alcohols from alkenes and water: Directed evolution of a styrene hydratase. *Angew. Chem. Int. Ed.* **62**, e202215093 (2023).

13 Horz, P. *et al.* Regioselective hydration of terpenes with cofactor-independent carotenoid 1,2-hydratase. *Angew. Chem. Int. Ed.* **64**, e202505942 (2025).

14 Zombeck, A., Hamilton, D. E. & Drago, R. S. Novel catalytic oxidations of terminal olefins by cobalt(II)-Schiff base complexes. *J. Am. Chem. Soc.* **104**, 6782–6784 (1982).

15 Mukaiyama, T. *et al.* Oxidation-reduction hydration of olefins with molecular oxygen and 2-propanol catalyzed by bis(acetylacetonato)cobalt(II). *Chem. Lett.* **18**, 449–452 (2006).

16 Inoki, S. *et al.* Bis(trifluoroacetylacetonato)cobalt(II) catalyzed oxidation-reduction hydration of olefins selective formation of alcohols from olefins. *Chem. Lett.* **18**, 515–518 (2006).

17 Wu, J. & Ma, Z. Metal-hydride hydrogen atom transfer (MHAT) reactions in natural product synthesis. *Org. Chem. Front.* **8**, 7050–7076 (2021).

18 Crossley, S. W. M., Obradors, C., Martinez, R. M. & Shenvi, R. A. Mn-, Fe-, and Co-catalyzed radical hydrofunctionalizations of olefins. *Chem. Rev.* **116**, 8912–9000 (2016).

19 Bhunia, A., Bergander, K., Daniliuc, C. G. & Studer, A. Fe-catalyzed anaerobic mukaiyama-type hydration of alkenes using nitroarenes. *Angew. Chem. Int. Ed.* **60**, 8313–8320 (2021).

20 Iwasaki, K., Wan, K. K., Oppedisano, A., Crossley, S. W. M. & Shenvi, R. A. Simple, chemoselective hydrogenation with thermodynamic stereocontrol. *J. Am. Chem. Soc.* **136**, 1300–1303 (2014).

21 Crossley, S. W. M., Barabé, F. & Shenvi, R. A. Simple, chemoselective, catalytic olefin isomerization. *J. Am. Chem. Soc.* **136**, 16788–16791 (2014).

22 Sato, M., Gunji, Y., Ikeno, T. & Yamada, T. Stereoselective preparation of α-hydroxycarboxamide by manganese complex catalyzed hydration of α,β-unsaturated carboxamide with molecular oxygen and phenylsilane. *Chem. Lett.* **33**, 1304–1305 (2004).

23 Yamada, T. Enantioselective borohydride reduction catalyzed by cobalt complexes: Discovery, analysis, and design for a halogen-free system. *Synth.*, 1628–1640 (2008).

24 Van Stappen, C. *et al.* Designing artificial metalloenzymes by tuning of the environment beyond the primary coordination sphere. *Chem. Rev.* **122**, 11974–12045 (2022).

25 Wang, J., Yin, Y., Zhang, Q., Zhang, W.-D. & Li, J. Artificial farnesol epoxidase enables a concise synthesis of meroterpenoids. *Science* **389**, 732–735 (2025).

26 Hammer, S. C., Marjanovic, A., Dominicus, J. M., Nestl, B. M. & Hauer, B. Squalene hopene cyclases are protonases for stereoselective Brønsted acid catalysis. *Nat. Chem. Biol.* **11**, 121–126 (2015).

27 Roy, S. *et al.* Stereoselective construction of β-, γ- and δ-lactam rings via enzymatic C–H amidation. *Nat. Catal.* **7**, 65–76 (2024).

28 Zhou, Q., Chin, M., Fu, Y., Liu, P. & Yang, Y. Stereodivergent atom-transfer radical cyclization by engineered cytochromes P450. *Science* **374**, 1612–1616 (2021).

29 Rui, J. Y. *et al.* Directed evolution of nonheme iron enzymes to access abiological radical-relay C(sp^3)-H azidation. *Science* **376**, 869–874 (2022).

30 Zhao, B. *et al.* Electricity-driven enzymatic dynamic kinetic oxidation. *Nature* **643**, 699–704 (2025).

31 Ouyang, Y., Turek-Herman, J., Qiao, T. & Hyster, T. K. Asymmetric carbohydroxylation of alkenes using photoenzymatic catalysis. *J. Am. Chem. Soc.* **145**, 17018–17022 (2023).

32 Hammer, S. C. *et al.* Anti-Markovnikov alkene oxidation by metal-oxo–mediated enzyme catalysis. *Science* **358**, 215–218 (2017).

33 Gergel, S. *et al.* Engineered cytochrome P450 for direct arylalkene-to-ketone oxidation via highly reactive carbocation intermediates. *Nat. Catal.* **6**, 606–617 (2023).

34 Roos, C. B. *et al.* Synthesis of enantioenriched atropisomers by biocatalytic deracemization. *Nature* **647**, 648–655 (2025).

35 Schwizer, F. *et al.* Artificial metalloenzymes: Reaction scope and optimization strategies. *Chem. Rev.* **118**, 142–231 (2018).

36 Chen, K. & Arnold, F. H. Engineering new catalytic activities in enzymes. *Nat. Catal.* **3**, 203–213 (2020).

37 Emmanuel, M. A. *et al.* Photobiocatalytic strategies for organic synthesis. *Chem. Rev.* **123**, 5459–5520 (2023).

38 Jain, S., Ospina, F. & Hammer, S. C. A new age of biocatalysis enabled by generic activation modes. *JACS Au* **4**, 2068–2080 (2024).

39 Wang, B. *et al.* Repurposing iron- and 2-oxoglutarate-dependent oxygenases to catalyze olefin hydration. *Angew. Chem. Int. Ed.* **62**, e202311099 (2023).

40 Li, J., Kumar, A. & Lewis, J. C. Non-native intramolecular radical cyclization catalyzed by a B12-dependent enzyme. *Angew. Chem. Int. Ed.* **62**, e202312893 (2023).

41 Ji, P., Park, J., Gu, Y., Clark, D. S. & Hartwig, J. F. Abiotic reduction of ketones with silanes catalysed by carbonic anhydrase through an enzymatic zinc hydride. *Nat. Chem.* **13**, 312–318 (2021).

42 Chen, R., Kayrouz, C. S., McAmis, E., Clark, D. S. & Hartwig, J. F. Carbonic anhydrase variants catalyze the reduction of dialkyl ketones with high enantioselectivity. *Angew. Chem. Int. Ed.* **63**, e202407111 (2024).

43 Chen, D. *et al.* An evolved artificial radical cyclase enables the construction of bicyclic terpenoid scaffolds via an H-atom transfer pathway. *Nat. Chem.* **16**, 1656–1664 (2024).

44 Zhang, X. *et al.* Repurposing myoglobin into an abiological asymmetric ketoreductase. *Chem* **10**, 2577–2589 (2024).

45 Wan, Z. *et al.* Stereoconvergent reduction of alkenes using a repurposed iron-based dioxygenase. *Nat. Synth.* **4**, 976–986 (2025).

46 Zhang, X., Chen, D., Álvarez, M. & Ward, T. R. Repurposing haemoproteins for asymmetric metal-catalysed H atom transfer. *Nature* **644**, 381–390 (2025).

47 Vallapurackal, J. *et al.* Biocatalytic, asymmetric radical hydrogenation of unactivated alkenes. *Science* **390**, 1050–1056 (2025).

48 Perkins L, M. C., Rourke M, Gardner R, Hall R, Brunold T, Buller A. Enzymatic metal-hydrogen atom transfer with a cobalt protoporphyrin cofactor. *ChemRxiv* (2024).

49 Wang, W. *et al.* Manganese transfer hydrogenases based on the biotin-streptavidin technology. *Angew. Chem. Int. Ed.* **62**, e202311896 (2023).

50 Cui, D. *et al.* Metalloenzyme-catalyzed asymmetric transfer hydrogenation for the synthesis of chiral amines. *Angew. Chem. Int. Ed.* **64**, e202511298 (2025).

51 Fansher, D. J., Besna, J. N., Fendri, A. & Pelletier, J. N. Choose your own adventure: A comprehensive database of reactions catalyzed by cytochrome P450 BM3 variants. *ACS Catal.* **14**, 5560–5592 (2024).

52 Azam, F. & Adler, M. J. Evaluating the aqueous stability of alkyl-/aryl-hydrosilanes by NMR spectroscopy and GC-MS. *ChemPlusChem* **90**, e202500310 (2025).

53 Vanhessche, K. P. M. & Sharpless, K. B. Ligand-dependent reversal of facial selectivity in the asymmetric dihydroxylation. *J. Org. Chem.* **61**, 7978–7979 (1996).

54 Wan, Z.-K. *et al.* Synthesis of potent and orally efficacious 11β-hydroxysteroid dehydrogenase type 1 inhibitor HSD-016. *J. Org. Chem.* **76**, 7048–7055 (2011).

55 Wayner, D. D. M., McPhee, D. J. & Griller, D. Oxidation and reduction potentials of transient free radicals. *J. Am. Chem. Soc.* **110**, 132–137 (1988).

56 Gutmann, V., Gritzner, G. & Danksagmuller, K. Solvent effects on the redox potential of hexacyanoferrate(III)-hexacyanoferrate(II). *Inorg. Chim. Acta* **17**, 81–86 (1976).

57 Bosnidou, A. E. *et al.* Tandem $InCl_3$-promoted hydroperoxide rearrangements and nucleophilic additions: A straightforward entry to benzoxacycles. *J. Org. Chem.* **88**, 9277–9282 (2023).

58 Poulos, T. L. Heme enzyme structure and function. *Chem. Rev.* **114**, 3919–3962 (2014).

59 Thompson, J. A. & Wand, M. D. Interaction of cytochrome P-450 with a hydroperoxide derived from butylated hydroxytoluene. Mechanism of isomerization. *J. Biol. Chem.* **260**, 10637–10644 (1985).

60 Oliw, E. H. Fatty acid dioxygenase-cytochrome P450 fusion enzymes of filamentous fungal pathogens. *Fungal Genet. Biol.* **157**, 103623 (2021).

Supplementary Files

This is a list of supplementary files associated with this preprint. Click to download.

- P450radicalhydratasesupportinginformation.pdf